PHYSICAL REVIEW A VOLUME 24, NUMBER 3 SEPTEMBER 1981

Positron bremsstrahlung

I. J. Feng, R. H. Pratt, and H. K. Tseng*
Department of Physics and Astronomy, University of Pittsburgh, Pittsburgh, Pennsylvania 15260
(Received 13 March 1981)

Numerical results from a calculation of the positron bremsstrahlung spectrum in a partial-wave expansion are presented for $Z = 8$, 92 at photon energies 10, 50, and 500 keV. Data are presented both for a point-Coulomb potential and for a screened Hartree-Slater central potential. Comparison is made with the corresponding electron bremsstrahlung. In the point-Coulomb case the nonrelativistic Sommerfeld formula or the Elwert factor provides a quantitative prediction of the ratio of the two spectra for $Z = 8$, qualitative for $Z = 92$; similar accuracy is achieved in the screened case with a ratio of screened normalization. The positron spectrum is strongly suppressed for low-energy positrons, which cannot penetrate toward the repulsive central potential. For high-energy positrons or long-distance interactions the positron spectrum approaches the electron spectrum.

I. INTRODUCTION

We wish to report a preliminary study of the spectrum of positron bremsstrahlung. There is rather little distinction between the presence of a high-energy electron or positron in the field of an atom, except for the relatively rare events in which a high-energy positron annihilates an atomic electron.[1] But there is a substantial difference for low energies. As the energy of the incident and final projectile increases, the spectra of radiation from positrons and from electrons become increasingly similar. But for low energies the two spectra are dramatically different, representing an opposite response to a positive nuclear charge screened by a negative charge distribution of atomic electrons. A low-energy positron approaches the nucleus only to the extent that it is screened, while the approach of an electron is inhibited by the screening. For sufficiently low energies the atom appears as a neutral object to both projectiles, so that in both cases the amount of radiation decreases as the energy diminishes. This study is, in part, motivated by recent interest[2] in the observation of positron bremsstrahlung; such experiments are very sensitive to the nature and details of the screening of the nucleus by underlying mechanisms of the bremsstrahlung process and the extent to which they can be characterized by simpler analytic approaches. The study complements our earlier presentation[3,4] of results for the electron bremsstrahlung spectrum.

Our work is based on the code which we had previously developed[5] for the calculation of electron bremsstrahlung, described as a relatively simple electron transition in a self-consistent screened central potential, through the numerical determination of radial matrix elements resulting from a partial-wave expansion of the projectile and radiation wave functions. We present in the next section our results for the positron (and corresponding electron) spectrum for low-Z (oxygen, $Z=8$) and high-Z (uranium, $Z=92$) elements, both for a point-Coulomb and for a screened potential, for incident projectile energies T_1 of 10, 50, and 500 keV, and for fractions k/T_1 of incident projectile kinetic energy radiated $k/T_1 = 0.0$, 0.2, 0.4, 0.6, 0.8, and 0.9. (For $k/T_1 = 0$ we utilize the low-energy theorem[6] and a separate code for electron scattering.) We also present the predictions of several simpler analytic approaches. Then in Sec. III we focus our attention on the prediction of the *ratio* of positron to electron radiation, which helps to clarify the problems and the achievements of the simpler approaches.

II. POSITRON BREMSSTRAHLUNG

We present in Table I our numerical results for scaled relativistic positron and electron bremsstrahlung cross sections $\sigma(k) = \beta_1^2(k/Z^2)(d\sigma/dk)$, both for neutral ["exact" screened (ES)][7] and totally ionized ["exact" Coulomb (EC)] atoms. Here, $\beta_1 \equiv v_1/c$ is the incident electron or positron velocity. In our discussion we will often find it helpful to focus on the two endpoints of the bremsstrahlung spectrum: the *tip* ($k/T_1 = 1$), where all the kinetic energy of the projectile is radiated, and the soft-photon limit ($k/T_1 = 0$), where almost none of the energy is radiated. Most properties of the spectrum can be understood if we understand the properties of these two end points. We can see from our data that there are both differences and similarities between the positron bremsstrahlung spectrum $\sigma_+(k)$ and the electron bremsstrahlung spectrum $\sigma_-(k)$.

A. Point-Coulomb case

For given Z and T_1, due to the Coulomb repulsion of positrons, $\sigma_+(k)$ starts from zero at the

TABLE I. Electron (σ_-) and positron (σ_+) bremsstrahlung spectra $\beta_1^2(k/Z^2)(d\sigma/dk)$ (in mb) and their ratio, for oxygen ($Z=8$) and uranium ($Z=92$), for incident kinetic energies of 10, 50, and 500 keV, as a function of the fraction k/T_1 of incident energy radiated, both in a Coulomb (EC) and screened (ES) potential. Numbers in parentheses denote powers of ten.

T_1 (keV) \ k/T_1			$Z=8$						$Z=92$					
			0.0	0.2	0.4	0.6	0.8	0.9	0.0	0.2	0.4	0.6	0.8	0.9
10	(σ_+)	EC	∞			2.15	0.563	9.63(−2)	∞		1.40(−2)	2.85(−5)		
		ES	7.33			2.24	0.789	0.237	1.54		0.274	4.48(−2)	1.79(−3)	7.13(−5)
	(σ_-)	EC	∞			6.34	5.55	5.26	∞		7.05	6.68		
		ES	8.39		7.03	6.14	5.45	5.22	3.04		3.63	3.84	3.99	4.04
	$\left(\frac{\sigma_+}{\sigma_-}\right)$	EC	1.0			0.339	0.101	1.83(−2)	1.00		1.99(−3)	4.27(−6)		
		ES	0.874			0.365	0.145	4.54(−2)	0.507		7.55(−2)	1.17(−2)	4.49(−4)	1.77(−5)
50	(σ_+)	EC	∞		5.07	3.12	1.41	0.569	∞		0.452	2.81(−2)	5.76(−5)	
		ES	9.86	7.20	4.94	3.14	1.48	0.652	4.25	2.42	0.847	0.167	8.33(−3)	3.37(−4)
	(σ_-)	EC	∞		6.53	5.07	3.89	3.36	∞		7.94	7.32	6.90	6.73
		ES	10.5		6.43	5.01	3.86	3.33	6.67		6.18	5.91	5.72	5.64
	$\left(\frac{\sigma_+}{\sigma_-}\right)$	EC	1.0		0.776	0.615	0.362	0.169	1.00		5.69(−2)	3.84(−3)	8.35(−6)	
		ES	0.939		0.773	0.627	0.383	0.196	0.637		0.138	2.83(−2)	1.46(−3)	5.98(−5)
500	(σ_+)	EC	∞			2.68	1.38	0.769	∞		2.38	0.926	0.145	1.08(−2)
		ES	12.2	6.95	4.38	2.68	1.39	0.776	7.87	4.44	2.34	1.01	0.208	2.89(−2)
	(σ_-)	EC	∞			3.06	1.86	1.30	∞		7.21	5.72	4.70	4.27
		ES	12.6			3.04	1.86	1.29	11.7		6.56	5.16	4.35	3.99
	$\left(\frac{\sigma_+}{\sigma_-}\right)$	EC	1.00			0.876	0.742	0.592	1.00		0.330	0.162	3.09(−2)	2.53(−3)
		ES	0.968			0.882	0.747	0.602	0.673		0.356	0.196	4.78(−2)	7.24(−3)

tip ($k/T_1 = 1$), while $\sigma_-(k)$ starts from a finite value. Both $\sigma_+(k)$ and $\sigma_-(k)$ increase as k/T_1 decreases, and finally diverge logarithmically (with the same coefficient) in the soft-photon limit; this reflects the long-range character of the Coulomb potential and the coefficient is the same in all regions. In Table II we show the ratio of our results (EC) calculated with the partial-wave method and the result from the Sommerfeld (S) formula[8]

$$\sigma(k) = \frac{16\pi^2}{3}\alpha^3 \frac{1}{(e^{2\pi\nu_1}-1)(1-e^{-2\pi\nu_2})} X_0 \frac{d}{dX_0} \times |F(i\nu_1, i\nu_2; 1; X_0)|^2 , \quad (1)$$

with

$$\nu_i = Z\alpha/\beta_i, \quad X_0 = -\frac{4\nu_1\nu_2}{(\nu_1-\nu_2)^2} .$$

Here, F is the hypergeometric function. This result is obtained in dipole approximation with nonrelativistic quantum mechanics. Specifying $\nu_i = \pm Z\alpha/\beta_i$, it holds for both electrons and positrons. The predictions agree with our numerical results within 1–10% at 10 keV and remain fairly good at 50 keV, both for positrons and electrons and for light and heavy elements. The predictions are still qualitatively correct at 500 keV. This usefulness of the Sommerfeld formula for σ (which omits relativistic, retardation, and higher multipole effects) may be connected to the fact that at the soft-photon end of the spectrum all formulas for σ give the same prediction, while the tip of the spectrum is related to atomic photoeffect, for which[9] the same cancellation of relativistic and higher multipole effects has been observed. Note that there are two versions of Sommerfeld's results: the result calculated from Eq. (1) with relativistic kinematics,[10] i.e.,

$$\beta_i = P_i/E_i, \quad P_i = (E_i^2 - 1)^{1/2}, \quad E_i = 1 + T_i ,$$

TABLE II. Ratios of numerically calculated bremsstrahlung spectra (EC) and (ES) as defined in Table I to the corresponding predictions from the Sommerfeld formula (S), the Born-Elwert approximation (BE), the Born-Elwert-form-factor approximation (BEF), as well as ratios of (σ_+/σ_-) ratios to the Sommerfeld (S) and normalization (Norm) predictions.

T_1 (keV) \ k/T_1		$Z=8$ 0.0	0.2	0.4	0.6	0.8	0.9	$Z=92$ 0.0	0.2	0.4	0.6	0.8	0.9
10	(σ_+) S/EC	1.00			1.02	1.02	1.02	1.00		0.971	0.926		
	(σ_+) BE/EC	1.00			1.01	0.995	1.04	1.00					
	(σ_+) BEF/ES	1.09			0.880	0.669	0.383	1.23		$\ll 1$	$\ll 1$	$\ll 1$	
	(σ_-) S/EC	1.00			1.02	1.03	1.03	1.00		0.955	0.952		
	(σ_-) BE/EC	1.00			0.995	0.991	0.989	1.00		1.14			
	(σ_-) BEF/ES	0.950			0.935	0.941	0.939	1.84		1.41	1.30		
	$\left(\frac{\sigma_+}{\sigma_-}\right)$ S/EC	1.00			1.00	1.00	1.00	1.00		1.02	0.972		
	$\left(\frac{\sigma_+}{\sigma_-}\right)$ Norm/ES	1.14			1.04	0.945	0.877	1.97		1.23	1.17	1.20	1.31
50	(σ_+) S/EC	1.00		1.09	1.11	1.13	1.14	1.00		1.01	0.943	0.845	
	(σ_+) BE/EC	1.00		1.01	1.01	1.01	1.00	1.00		1.17			
	(σ_+) BEF/ES							1.81			0.171	$\ll 1$	$\ll 1$
	(σ_-) S/EC	1.00		1.08	1.11	1.14	1.16	1.00		0.923	0.923	0.928	0.930
	(σ_-) BE/EC	1.00		0.988	0.984	0.985	0.982	1.00		0.928	0.857	0.800	0.773
	(σ_-) BEF/ES							1.15			0.960	0.893	
	$\left(\frac{\sigma_+}{\sigma_-}\right)$ S/EC	1.00		1.01	1.00	0.989	0.988	1.00		1.09	1.02	0.911	
	$\left(\frac{\sigma_+}{\sigma_-}\right)$ Norm/ES	1.07		1.03	0.990	0.971	0.934	1.57		1.10	1.03	0.911	0.878
500	(σ_+) S/EC	1.00			1.59	1.81	1.94	1.00		1.37	1.30	1.05	0.831
	(σ_+) BE/EC	1.00			1.03	1.03	1.03	1.00		1.26	1.20	1.03	
	(σ_+) BEF/ES	0.954			1.08	1.02	1.02	1.24			1.05	0.720	
	(σ_-) S/EC	1.00			1.62	1.86	2.02	1.00		1.08	1.21	1.34	1.43
	(σ_-) BE/EC	1.00			1.00	0.973	0.962	1.00		0.716	0.631	0.540	0.529
	(σ_-) BEF/ES	0.954			1.00	0.973	0.970	0.84			0.67	0.57	
	$\left(\frac{\sigma_+}{\sigma_-}\right)$ S/EC	1.00			0.981	0.974	0.961	1.00		1.26	1.07	0.780	0.581
	$\left(\frac{\sigma_+}{\sigma_-}\right)$ Norm/ES	1.03			0.974	0.979	0.959	1.49		1.23	1.00	0.741	0.557

and the result calculated from Eq. (1) with nonrelativistic kinematics, i.e.,

$$\beta_i = p_i, \quad \beta_i = \sqrt{2T_i}\ .$$

In general, we find that the nonrelativistic prediction is better, which reflects the cancellation of relativistic and higher multipole effect. The results presented in Table II are obtained using nonrelativistic kinematics. In the high T_i limit S_{NR} would predict that the electron tip $\sigma_-(k)$ vanishes; S_R correctly predicts that $\sigma_-(k)$ remains finite but gives the wrong constant, even to lowest order in $Z\alpha$.

The most widely used expressions for bremsstrahlung are based on Born approximation, which does not distinguish electron and positron bremsstrahlung. In nonrelativistic Born approximation $\sigma(k) = \frac{16}{3}\alpha^3 \ln[(p_1+p_2)/(p_1-p_2)]$; the considerably more complicated relativistic result is given by the Bethe-Heitler formula. These expressions, again exact in the soft-photon limit of the spectrum, vanish at the tip of the expression which for electrons is incorrect, owing to the incorrect characterization of the normalization of the outgoing low-energy electron. The results can be corrected if one multiplies by the Elwert factor[11] $f_E = (\nu_2/\nu_1)\,(1-e^{-2\pi\nu_1})/(1-e^{-2\pi\nu_2})$, the square of the ratio of final to initial continuum-wave-function normalization. The correct finite value to lowest order in $Z\alpha$ is obtained for the tip value of electron bremsstrahlung, while positron bremsstrahlung now vanishes exponentially. We show these Born-Elwert (BE) predictions for the electron and positron spectrum in Table II.

B. Screened case

In Figs. 1 and 2, as well as in the tables, we show the comparison of $\sigma_+(k)$ and $\sigma_-(k)$ for the screened case. The screened spectrum $\sigma_-(k)$ from a neutral atom lies below the point-Coulomb spectrum, i.e., the screening effect of atomic electrons reduces the cross section. In the screened case $\sigma_- = 0$ (due to the normalization factor) at the tip (contrasted with the finite point-Coulomb value) but rapidly rises in the first 5–50 eV[12,13]; it remains finite in the soft-photon limit (contrasted with the logarithmic divergence of the Coulomb case.) However, for $\sigma_+(k)$ the screened spectrum from a neutral atom lies below the point-Coulomb spectrum only near the soft-photon part of the spectrum, especially for low T_1 and high Z, again remaining finite in the soft-photon limit. Toward the tip end of the spectrum, atomic-electron screening increases the cross section, while as for electrons, $\sigma_+(k) = 0$ at the tip for the screened case. We may understand this crossover in the effects of screening on the positron spectrum in

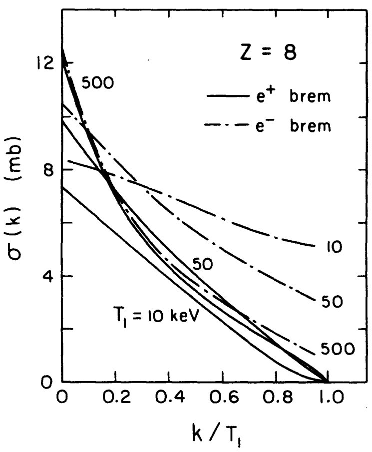

FIG. 1. Comparison of positron and electron bremsstrahlung energy spectra $\sigma(k)$ for $Z=8$; $T_1=10$, 50, and 500 keV.

terms of the regions in configuration space which determine the matrix element. At the soft-photon end of the spectrum the matrix element is determined at large distances, where the nuclear charge is now screened and so not available to accelerate the positron, thus reducing the cross section. At the tip of the spectrum the process is determined at smaller distances, to which a low-energy positron cannot penetrate in the repulsive nuclear Coulomb potential and penetrates better as the potential becomes screened. The resulting σ_+ is always smaller than σ_-; for given Z and T_1, $\sigma_+(k)$ deviates from $\sigma_-(k)$ more near the tip and this deviation increases as T_1 decreases and Z increases, as shown in Table I.

With screening, Born approximation is modified by a form factor, again the same for elec-

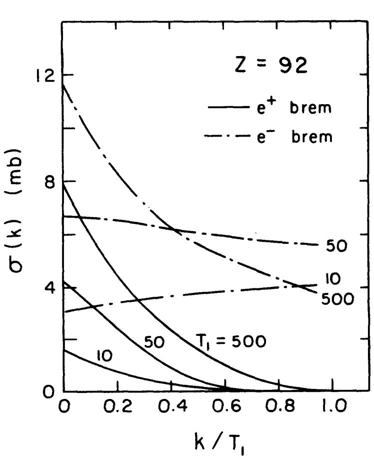

FIG. 2. Same as Fig. 1, except for $Z=92$.

trons and for positrons. The problems of incorrect behavior near the tip remain, and for electrons relatively good results (quantitative for low Z, qualitative for high Z) have been obtained by again multiplying by the Elwert factor. This Born-Elwert-form-factor (BEF) approach does not work as well for positrons, because the normalization of low-energy positrons deviates markedly from the Coulomb result to much higher energies. (See Table II.) This suggests the use of the ratio of screened rather than Coulomb normalizations, for which again either relativistic or nonrelativistic values may be used. As shown in the tables, this leads to predictions of an accuracy similar to that obtained in the Coulomb case, both for electrons and for positrons.

III. RATIO OF POSITRON TO ELECTRON BREMSSTRAHLUNG CROSS SECTIONS

It is instructive to focus some attention on the ratio of positron to electron bremsstrahlung cross sections, because this ratio serves to separate and emphasize certain features in the dynamics of the process while omitting others. In particular, the ratio only examines features which go beyond Born approximation and the form factor; in the ratio Sommerfeld formula, Elwert-Born, and Elwert-Born form factor all reduce to the simple prediction $e^{2\pi(\nu_1-\nu_2)}$, which may be compared with a ratio of the corresponding positron- and electron-screened normalizations. In the tables we show these ratios, our numerical Coulomb and screened results for these ratios, and finally also the ratios of numerical and normalization ratios. It should be noted that the ratio reduces to one for high-energy particles, as predicted by the normalization ratios, and also in the Coulomb case at the soft-photon end of the spectrum (where the screened normalization ratio prediction of unequal electron and positron cross sections is incorrect). By contrast, positron bremsstrahlung is suppressed for low-energy (final) positrons, because they are unable to come near the nuclear charge.

A. Point-Coulomb case

For the low-Z case ($Z=8$), in the energy range we considered in this paper, the point-Coulomb ratio σ_+/σ_- is very well predicted by the Sommerfeld (or Elwert) ratio $e^{2\pi(\nu_1-\nu_2)}$, as shown in Table II. For the high-Z case ($Z=92$) corrections to the ratio are important (especially with S_R) when T_1 is high, as shown in Table II. Nevertheless, for $Z=92$, the ratio σ_+/σ_- in the point-Coulomb case is still well predicted (within 10%) over most of the spectrum with S for T_1 up to 50 keV.

B. Screened case

There is an order of magnitude difference between S and the screened numerical ratio $\sigma_+(k)/\sigma_-(k)$, particularly for high Z, low T_1 at the hard-photon end, primarily because a low-energy positron normalization is much more sensitive to screening. A qualitatively better result (within a factor of 2) for all Z, all energy over the spectrum, for the ratio is obtained by using instead the screened S-wave normalization ratios of positrons and electrons $(N_{+2}N_{-1}/N_{-2}N_{+1})^2$, which, in fact, reduces in the point-Coulomb case to $e^{2\pi(\nu_1-\nu_2)}$, either relativistically or nonrelativistically. (Nonrelativistically, this is the full normalization of the three-dimensional continuum wave function at the origin, while relativistically p waves would also contribute to the full normalization.) Note that in the point-Coulomb case all partial waves have the same normalization ratio, while in the screened case the normalization ratio is l dependent, as shown in Fig. 3. (For large T_1 only final s and p waves contribute at the tip, while for low T_1 all final waves contribute.) For high Z ($Z=92$) and intermediate energies ($T_1=50$, 500 keV), S/EC and Norm/ES give similar re-

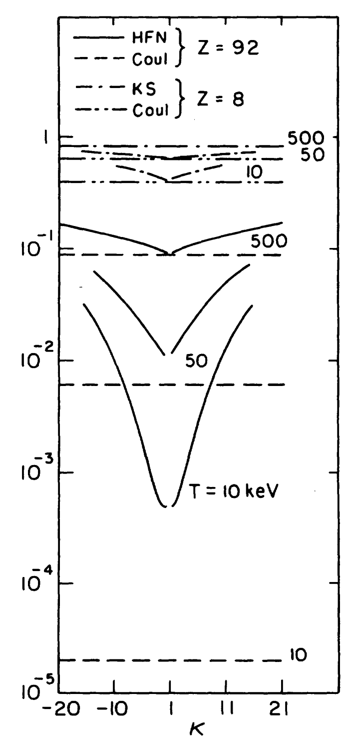

FIG. 3. Variation of the partial-wave normalization ratio $N_+(\kappa)/N_-(\kappa)$ of positrons and electrons with the quantum number κ. Here $\kappa=\pm(j+\frac{1}{2})$ as $j=l\pm\frac{1}{2}$, and l and j are quantum numbers of the orbital and total angular momentum of the electron or positron.

sults, except at the soft-photon end of spectrum where many partial waves contribute; the origin for the factor of 2 discrepancy for both Coulomb and screened cases remains unclear. For high Z and low T_1 ($T_1 = 10$ keV) the differences between Coulomb and screened results (poorer in the screened case) reflect the error made in the treatment of screening by taking normalization ratios of all partial waves to be the same. The high-Z case differences at the soft-photon end of the spectrum, which go beyond normalization effects, also remain unclear.

This work was supported in part by the National Science Foundation and the National Science Council of the Republic of China.

---

*Permanent address: Department of Physics, National Central University, Chung-Li, Taiwan, Republic of China.

[1]W. Heitler, *The Quantum Theory of Radiation* (Oxford University Press, London, 1954), Chap. 15; H. K. Tseng and R. H. Pratt, Phys. Rev. A 7, 1423 (1973).

[2]H. Kleinpoppen (private communication); S. Seltzer (private communication).

[3]C. M. Lee, L. Kissel, R. H. Pratt, and H. K. Tseng, Phys. Rev. A 13, 1714 (1976).

[4]R. H. Pratt, H. K. Tseng, C. M. Lee, L. Kissel, C. MacCallum, and M. Riley, At. Data Nucl. Data Tables 20, 175 (1977).

[5]H. K. Tseng and R. H. Pratt, Phys. Rev. A 3, 100 (1971).

[6]F. E. Low, Phys. Rev. 110, 974 (1958); T. H. Barnett and N. M. Kroll, Phys. Rev. Lett. 20, 86 (1968).

[7]For electron bremsstrahlung we used the Kohn-Sham (KS) potential, which includes an approximate exchange term which is not appropriate for positrons, and for positron bremsstrahlung we used a Hartree-Fock-Slater potential with the exchange term omitted (HFN); W. Kohn and L. S. Sham, Phys. Rev. 140, A1133 (1965); D. A. Liberman, T. B. Mann, and J. T. Waker, Comput. Phys. Commun. 2, 107 (1971).

[8]A. Sommerfeld, Ann. Phys. (Leipzig) 11, 257 (1931).

[9]S. D. Oh, J. McEnnan and R. H. Pratt, Phys. Rev. A 14, 1428 (1976).

[10]Note that we use units such that $\hbar = m = c = 1$.

[11]G. Elwert, Ann. Phys. (Leipzig) 34, 178 (1939).

[12]R. H. Pratt and H. K. Tseng, Phys. Rev. A 11, 1797 (1975).

[13]C. M. Lee and R. H. Pratt, Phys. Rev. A 12, 707 (1975).